

INVESTIGATION OF THE  $^{42}\text{Ca}(n, \gamma)^{43}\text{Ca}$  REACTION

H. GRUPPELAAR, A. M. F. OP DEN KAMP and A. M. J. SPITS

*Fysisch Laboratorium, Rijksuniversiteit, Utrecht, Nederland*

Received 17 March 1969

**Abstract:** Gamma rays from thermal-neutron capture in enriched  $^{42}\text{Ca}$  were investigated with Ge(Li) detectors. Gamma-gamma coincidence measurements were performed with a Ge(Li)-NaI detector combination. A decay scheme of  $^{43}\text{Ca}$  has been constructed containing 42 of the 47 observed  $\gamma$ -lines. The excitation energies of 16 levels of  $^{43}\text{Ca}$  were determined with uncertainties of 0.2 to 1.1 keV. The  $^{42}\text{Ca}(n, \gamma)$  reaction  $Q$ -value is  $Q = 7932.7 \pm 0.5$  keV. From the  $\gamma$ -decay,  $J^\pi = \frac{3}{2}^-$  can be assigned to the  $I_n(d, p) = 1$  level at  $E_x = 2046$  keV. A strong correlation between the  $(n, \gamma)$  and  $(d, p)$  strengths was found.

E

NUCLEAR REACTIONS  $^{42}\text{Ca}(n, \gamma)$ ,  $E = \text{thermal}$ ; measured  $E_\gamma$ ,  $I_\gamma$ ,  $\gamma$ - $\gamma$  coin; deduced  $Q$ .  $^{43}\text{Ca}$  deduced levels,  $\gamma$ -branching,  $J$ . Enriched target, Ge(Li) detector.

## 1. Introduction

Gamma rays from thermal-neutron capture in  $^{42}\text{Ca}$  have been studied with NaI crystals by Cranston, White and Smith <sup>1</sup>). As can be seen from the review article of Endt and Van der Leun <sup>2</sup>), only a few  $\gamma$ -rays could be fitted into the level scheme of  $^{43}\text{Ca}$ . The present work is a continuation of previous investigations with Ge(Li) detectors on the  $\gamma$ -rays from thermal-neutron capture in the even calcium isotopes <sup>3,4</sup>).

Recently, Chasman, Jones and Ristinen <sup>5</sup>) investigated the  $\gamma$ -rays from the  $^{43}\text{Ca}$   $(p, p'\gamma)$  reaction and from the  $\beta^-$  decay of  $^{43}\text{K}$  with a Ge(Li) detector. These authors presented a decay scheme of  $^{43}\text{Ca}$  with excitation energies up to 2.25 MeV. Gamma rays following the  $\beta^-$  decay of  $^{43}\text{K}$  have also been reported recently by Larson and Gordon <sup>6</sup>).

The energy levels of  $^{43}\text{Ca}$  have been extensively studied by means of the  $^{43}\text{Ca}$   $(p, p')$ ,  $^{43}\text{Ca}(d, d')$ ,  $^{42}\text{Ca}(d, p)$ ,  $^{44}\text{Ca}(^3\text{He}, \alpha)$ ,  $^{41}\text{K}(^3\text{He}, p)$  and  $^{44}\text{Ca}(p, d)$  reactions [refs. <sup>5,7-11</sup>]. Since the  $\gamma$ -decay of most of these states was unknown, it was thought that a study of the  $^{42}\text{Ca}(n, \gamma)$  reaction would be worthwhile. In particular the branching ratios of the  $\gamma$ -ray transitions may be useful because of the considerable theoretical interest in the shell-model structure of the calcium isotopes <sup>12-17</sup>).

The experimental arrangement, which will be described below, is particularly suited for the recording of  $\gamma$ -ray spectra from thermal-neutron capture in small amounts of enriched isotopes. The minimum quantity of target material needed is in the order of 50 mg for samples with a thermal-neutron cross section of 1 b.

## 2. Experimental arrangement

A beam of thermal neutrons was obtained with a neutron filter, placed in one of the radial beam holes of the Dutch High Flux Reactor. This neutron filter consisted of quartz and bismuth single crystals and was cooled down to the temperature of liquid nitrogen. The thermal-neutron flux at the place of the target was about  $10^7 \text{ cm}^{-2} \cdot \text{s}^{-1}$ . This set-up has been described in more detail by Van Middelkoop and Spilling<sup>18)</sup>.

The  $\gamma$ -rays were detected with a  $6.5 \text{ cm}^3$  planar Ge(Li) detector from Philips and an Ortec  $23 \text{ cm}^3$  coaxial detector. The electronics consisted of an Ortec 118A pre-amplifier, a main amplifier from Nuclear Enterprises and a Laben 4096-channel pulse-height analyser. The linearity of the system was tested with a precision pulse generator. The maximum deviation from linearity was 0.9 channel for channels 100 to 4000. The overall resolution of the system with the  $23 \text{ cm}^3$  Ge(Li) detector, measured over three days, was 3.3 keV for 1.33 MeV  $\gamma$ -rays and 7.5 keV for 5.0 MeV  $\gamma$ -rays.

TABLE 1  
Isotopic composition of the  $^{42}\text{Ca}$  sample

Isotope	Abundance ( $P$ ) <sup>a)</sup>	$\sigma$ <sup>b)</sup>	$P \times \sigma$ (b)
$^{40}\text{Ca}$	35.15	$0.22 \pm 0.04$ b	7.7
$^{42}\text{Ca}$	63.90	$0.70 \pm 0.16$ b	44.7
$^{43}\text{Ca}$	0.24	$6.2 \pm 1.1$ b	1.5
$^{44}\text{Ca}$	0.68	$1.1 \pm 0.2$ b	0.8
$^{46}\text{Ca}$	0.005	$0.25 \pm 0.10$ b	0.001
$^{48}\text{Ca}$	0.02	$1.1 \pm 0.1$ b	0.2
$^{12}\text{C}$	100	$3.4 \pm 0.3$ mb	0.3
$^1\text{H}$	$\approx 100$	$332 \pm 2$ mb	$\approx 33$
$^{113}\text{Cd}$	$\approx 4 \times 10^{-4}$	$20.0 \pm 0.3$ kb	$\approx 8$
$^{149}\text{Sm}$	$\approx 1 \times 10^{-4}$	$40.8 \pm 0.9$ kb	$\approx 5$
$^{157}\text{Gd}$	$\approx 3 \times 10^{-5}$	$240 \pm 12$ kb	$\approx 7$

<sup>a)</sup> Per 100 Ca atoms.

<sup>b)</sup> Thermal-neutron cross sections. The cross sections for  $^{42,43,44}\text{Ca}$  are from ref. <sup>20)</sup>, the others from ref. <sup>21)</sup>.

With the  $23 \text{ cm}^3$  Ge(Li) detector and a  $12.7 \times 12.7 \text{ cm}$  NaI crystal some  $\gamma$ - $\gamma$  coincidence measurements were performed. The coincidence system had a time resolution of  $2\tau = 50 \text{ ns}$ . Less than 7% of the coincident pulses were due to random events. With a digital-window discriminator<sup>19)</sup>, routing the subgroups of the memory of the analyser, four windows were placed on the pulse-height spectrum from the NaI crystal. Two runs, each with a counting time of about 60 h, were performed.

The carbonate target, which contained 80 mg of calcium, was enclosed in a teflon cylinder. The isotopic composition of the sample, which was on loan from the Electromagnetic Separation Group at Harwell, is shown in table 1. In this sample, traces of some elements with exceptionally high thermal-neutron capture cross sections were detected, which are also listed in table 1.

The main contribution to the background radiation came from thermal-neutron capture in the teflon target holder ( $^{19}\text{F}$ ) and in  $^{14}\text{N}$ ,  $^{207}\text{Pb}$  and  $^{56}\text{Fe}$ . The background radiation was investigated separately with a "dummy target", consisting of an identical target holder, filled with the same amount of natural  $\text{CaCO}_3$  as present in the enriched sample. Each recording of a  $\gamma$ -spectrum with the enriched sample was followed by one with the dummy target. The latter spectrum was subtracted from the previous one, after corrections for zero-point and gain shifts. The spectrum, measured with the dummy target, was normalized such, that the intensities of the most important background  $\gamma$ -rays (due to capture in  $^{19}\text{F}$ ) were about equal to those in the spectrum, measured with the  $^{42}\text{Ca}$  sample.

With both Ge(Li) detectors  $\gamma$ -ray spectra were measured in the ranges  $E_\gamma = 0\text{-}7$  MeV and  $0.1\text{-}2.4$  MeV. To provide a good energy calibration a separate run was made with graphite added to the  $^{42}\text{Ca}$  sample, while in the range  $E_\gamma = 0.1\text{-}2.4$  MeV the  $\gamma$ -rays of some radioactive sources were measured simultaneously. Each recording of a  $\gamma$ -ray spectrum took 3-4 days.

### 3. Analysis of measurements ¶¶

The peak positions were determined by fitting Gaussian functions to the peaks. The identification of the peaks was facilitated by the fact that the  $\gamma$ -ray spectra were measured with two Ge(Li) detectors of different sizes. As a consequence, the chance that a double-escape peak has been interpreted as a full-energy peak (or the opposite) was reduced appreciably. In all figures and tables in this paper only the results obtained with the larger detector will be shown, because of the somewhat better statistics of the spectra obtained with this detector.

The efficiency curves for full-energy, single- and double-escape peaks were determined by means of calibrated radioactive sources and the  $^{12}\text{C}(n, \gamma)$  and  $^{53}\text{Cr}(n, \gamma)$  reactions<sup>22,23</sup>). In addition, several other  $(n, \gamma)$  reactions were used to determine the efficiencies of escape peaks relative to full-energy peaks.

In table 2 the energies of peaks are given, which were used for the energy calibration of the low-energy spectrum and the spectrum, measured with graphite added to the  $^{42}\text{Ca}$  sample.

In the case of the low-energy spectrum, a third-degree polynomial was fitted through the nine calibration points. The standard deviation between energies, calculated from the calibration curve, and the calibration energies was 0.06 keV. The energies of nearly all  $\gamma$ -rays with  $E_\gamma < 2.4$  MeV were determined in this way.

A fourth-degree polynomial was fitted through the 11 calibration points of the second spectrum, with a standard deviation of 0.09 keV. From this spectrum resulted the energies of the most prominent  $\gamma$ -rays with  $E_\gamma > 2$  MeV. The weaker  $\gamma$ -lines and those which were obscured by calibration  $\gamma$ -lines, were in turn determined from the spectrum in the range  $E_\gamma = 0\text{-}7$  MeV, using the best-determined energies from the two calibration spectra.

TABLE 2  
Energies of  $\gamma$ -rays used for calibration

$E_\gamma = 0.1\text{-}2.4$ MeV			$E_\gamma = 0.5\text{-}5.0$ MeV		
isotope <sup>a)</sup>	$E_\gamma$ (keV)	ref.	isotope <sup>a)</sup>	$E_\gamma$ (keV)	ref.
$^{57}\text{Co}$ (r)	122.05 $\pm$ 0.05	<sup>35)</sup>	annihilation	511.006 $\pm$ 0.002	<sup>35)</sup>
annihilation	511.006 $\pm$ 0.002	<sup>35)</sup>	$^2\text{H}$ (d)	1201.339 $\pm$ 0.046	<sup>34)</sup>
$^{60}\text{Co}$ (r)	1173.226 $\pm$ 0.040	<sup>35)</sup>	$^{13}\text{C}$	1261.76 $\pm$ 0.07	<sup>36)</sup>
$^2\text{H}$ (d)	1201.339 $\pm$ 0.046	<sup>34)</sup>	$^2\text{H}$ (s)	1712.345 $\pm$ 0.046	<sup>34)</sup>
$^{13}\text{C}$	1261.76 $\pm$ 0.07	<sup>36)</sup>	$^2\text{H}$	2223.351 $\pm$ 0.046	<sup>34)</sup>
$^{60}\text{Co}$ (r)	1332.483 $\pm$ 0.046	<sup>35)</sup>	$^{13}\text{C}$ (d)	2661.71 $\pm$ 0.14	<sup>36)</sup>
$^2\text{H}$ (s)	1712.345 $\pm$ 0.046	<sup>34)</sup>	$^{13}\text{C}$ (s)	3172.72 $\pm$ 0.14	<sup>36)</sup>
$^{88}\text{Y}$ (r)	1836.08 $\pm$ 0.07	<sup>35)</sup>	$^{13}\text{C}$	3683.72 $\pm$ 0.14	<sup>36)</sup>
$^2\text{H}$	2223.351 $\pm$ 0.046	<sup>34)</sup>	$^{13}\text{C}$ (d)	3923.01 $\pm$ 0.15	<sup>36)</sup>
			$^{13}\text{C}$ (s)	4434.02 $\pm$ 0.15	<sup>36)</sup>
			$^{13}\text{C}$	4945.02 $\pm$ 0.15	<sup>36)</sup>

<sup>a)</sup> The symbols (d) and (s) denote "double"- and "single"-escape peaks, respectively, and (r) radioactive source.

#### 4. Results

In fig. 1 the background-subtracted spectrum of the  $^{42}\text{Ca}(n, \gamma)^{43}\text{Ca}$  reaction, measured with the 23 cm<sup>3</sup> Ge(Li) detector is shown. The peaks are labelled with unprimed, primed or doubly-primed energies in keV, indicating full-energy, single- or double-escape peaks, respectively. Residual peaks or peaks due to contamination of the target are labelled with the corresponding final nucleus or with the symbol "Bgr", if the peak could not be identified.

The energies and intensities of  $\gamma$ -rays assigned to  $^{43}\text{Ca}$  are listed in table 3. The intensities are normalized such that the sum of the intensities of  $\gamma$ -rays de-exciting to the ground state is 100. This normalization leads to relative intensities of the  $\gamma$ -rays which are about equal to the number of photons per 100 captures. The alternative normalization, which requires that the total intensity of all primary  $\gamma$ -rays equals 100, was not used here because (i) the total intensity of all primary  $\gamma$ -rays is less than the total intensity reaching the ground state, which might indicate that some primary  $\gamma$ -rays are missing, (ii) the number of  $\gamma$ -transitions to the ground state is far less than the number of primary  $\gamma$ -rays and (iii) no systematic errors are present in the efficiency curves for  $E_\gamma < 3$  MeV.

Some  $\gamma$ - $\gamma$  coincidence spectra are shown in fig. 2. In table 4 the results of these measurements are summarized. The spectra corresponding to gate 1 and 2 (see table 4) are completely shown in fig. 2, while from the other spectra only those peaks are shown, which were not observed in the spectrum corresponding to the preceding gate.

The decay scheme of  $^{43}\text{Ca}$  is presented in fig. 3. Here the total primary intensity is normalized to 100. The  $\gamma$ -transitions in the decay scheme, which were observed in coincidence, are indicated by arrows starting with open circles. To facilitate the construction of the decay scheme, a computer program was written, which selects  $\gamma$ -

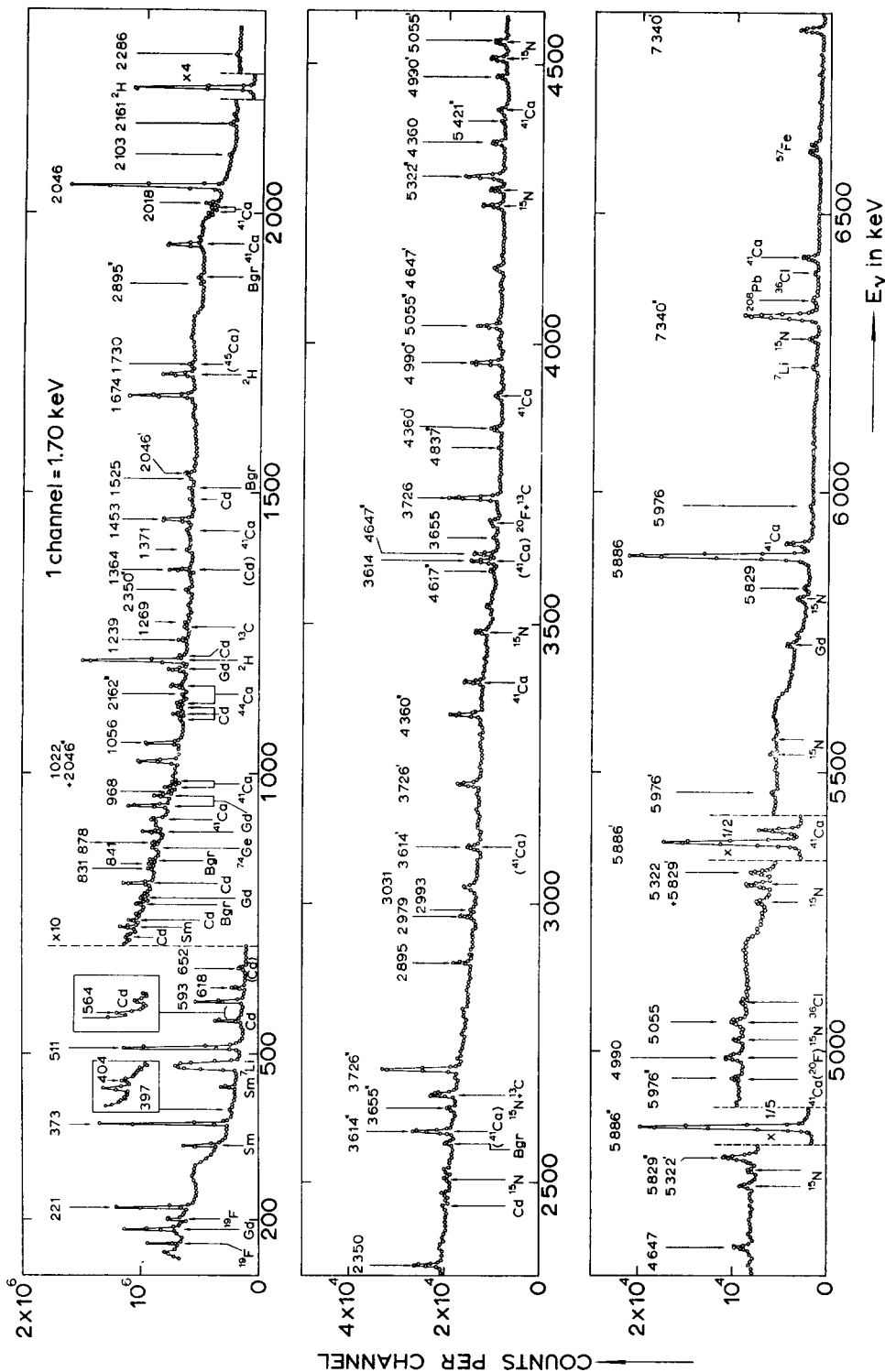


Fig. 1. Spectrum of the  $^{42}\text{Ca}(n, \gamma)^{43}\text{Ca}$  reaction after background subtraction. Peaks are labelled with unprimed, primed or doubly primed energies in keV, indicating full-energy, single- or double-escape peaks, respectively. Residual background peaks or peaks due to contamination of the target are labelled with the corresponding final nuclei or with the symbol "Bgr", if the peak could not be identified. In smooth regions in between peaks the mean of each four consecutive points is plotted.

TABLE 3  
Gamma rays observed in the  $^{42}\text{Ca}(n, \gamma)^{43}\text{Ca}$  reaction

$E_\gamma + E_r$ <sup>a)</sup> (keV)	Intensity <sup>b)</sup>	Interpretation <sup>c)</sup> ( $E_x$ in keV)	$E_\gamma + E_r$ <sup>a)</sup> (keV)	Intensity <sup>b)</sup>	Interpretation <sup>c)</sup> ( $E_x$ in keV)
$220.6 \pm 0.3$	$11 \pm 1$	$593 \rightarrow 373$	$2102.8 \pm 0.6$	$1.2 \pm 0.5$	$2103 \rightarrow 0$ <sup>f)</sup>
$372.7 \pm 0.2$	$38 \pm 4$	$373 \rightarrow 0$	$2161.2 \pm 0.6$	$2.1 \pm 0.3$	$4207 \rightarrow 2046$
$396.9 \pm 0.4$	$0.9 \pm 0.2$	$990 \rightarrow 593$	$2285.5 \pm 1.0$	$1.4 \pm 0.3$	$2878 \rightarrow 593$
$404.0 \pm 0.8$	$0.5 \pm 0.2$	$1394 \rightarrow 990$	$2350.4 \pm 0.4$	$2.5 \pm 0.3$	$2944 \rightarrow 593$
$564.4 \pm 0.6$	$1.5 \pm 0.5$	$2611 \rightarrow 2046$ <sup>d)</sup>	$2895.2 \pm 0.5$	$2.0 \pm 0.3$	C $\rightarrow$ 5038
$593.4 \pm 0.6$	$23 \pm 2$	$593 \rightarrow 0$	$2979.0 \pm 0.7$	$1.2 \pm 0.3$	$3573 \rightarrow 593$
$617.7 \pm 0.3$	$6.6 \pm 0.7$	$990 \rightarrow 373$	$2992.5 \pm 1.0$	$0.6 \pm 0.3$	$5038 \rightarrow 2046$
$651.6 \pm 0.6$	$0.9 \pm 0.5$	$2046 \rightarrow 1394$ <sup>e)</sup>	$3031.4 \pm 1.0$	$1.1 \pm 0.3$	C $\rightarrow$ 4902
$831.4 \pm 1.0$	$0.4 \pm 0.2$	$2878 \rightarrow 2046$			
$840.9 \pm 1.0$	$0.3 \pm 0.2$	$2944 \rightarrow 2103$	$3613.6 \pm 0.8$	$4.7 \pm 1.2$	$4207 \rightarrow 593$
$878.2 \pm 0.6$	$0.9 \pm 0.2$		$3654.9 \pm 0.6$	$0.9 \pm 0.3$	
$967.5 \pm 1.5$	$\approx 0.2$	$1958 \rightarrow 990$	$3725.5 \pm 0.3$	$8.3 \pm 1.2$	C $\rightarrow$ 4207
$1021.5 \pm 1.0$	$1.4 \pm 0.4$	$1394 \rightarrow 373$	$4359.7 \pm 0.5$	$2.9 \pm 0.4$	C $\rightarrow$ 3573
$1055.9 \pm 0.6$	$4.2 \pm 0.6$	$2046 \rightarrow 990$	$4616.9 \pm 0.9$	$0.6 \pm 0.3$	C $\rightarrow$ 3315
$1239.1 \pm 1.2$	$1.0 \pm 0.2$	$3286 \rightarrow 2046$	$4646.5 \pm 0.6$	$2.4 \pm 0.5$	C $\rightarrow$ 3286
$1268.9 \pm 0.6$	$0.7 \pm 0.2$	$3315 \rightarrow 2046$	$4837.1 \pm 0.9$	$\approx 0.1$	
$1363.9 \pm 1.0$	$1.5 \pm 1.0$	$1958 \rightarrow 593$	$4989.5 \pm 0.5$	$3.6 \pm 0.5$	C $\rightarrow$ 2944
$1370.5 \pm 1.0$	$1.1 \pm 0.2$		$5054.5 \pm 0.5$	$2.4 \pm 0.4$	C $\rightarrow$ 2878
$1453.0 \pm 0.3$	$4.9 \pm 0.5$	$2046 \rightarrow 593$	$5321.8 \pm 0.5$	$4.1 \pm 0.6$	C $\rightarrow$ 2611
$1525.4 \pm 1.0$	$0.7 \pm 0.2$	$3573 \rightarrow 2046$	$5421.1 \pm 1.2$	$\approx 0.2$	
$1673.5 \pm 0.4$	$11.9 \pm 1.2$	$2046 \rightarrow 373$	$5829.0 \pm 1.5$	$0.9 \pm 0.3$	C $\rightarrow$ 2103
$1729.9 \pm 1.0$	$1.2 \pm 0.4$	$2103 \rightarrow 373$	$5886.4 \pm 0.4$	$53 \pm 8$	C $\rightarrow$ 2046
$2017.9 \pm 0.8$	$2.8 \pm 0.3$	$2611 \rightarrow 593$	$5975.6 \pm 1.5$	$0.6 \pm 0.3$	C $\rightarrow$ 1958
$2046.4 \pm 0.3$	$38 \pm 4$	$2046 \rightarrow 0$	$7339.7 \pm 0.7$	$5.7 \pm 0.9$	C $\rightarrow$ 593

<sup>a)</sup> The recoil correction is denoted by  $E_r$ .

<sup>b)</sup> The sum of the intensities of  $\gamma$ -transitions proceeding to the ground state is normalized to 100. The relative intensities in column 2 are about equal to the number of photons per 100 captures.

<sup>c)</sup> The capturing state is denoted by C.

<sup>d)</sup> Coincidence measurements reject the alternative interpretation:  $1958 \rightarrow 1394$  keV.

<sup>e)</sup> Coincidence measurements reject the alternative interpretation:  $2611 \rightarrow 1985$  keV.

<sup>f)</sup> Alternative interpretation:  $4207 \rightarrow 2103$  keV.

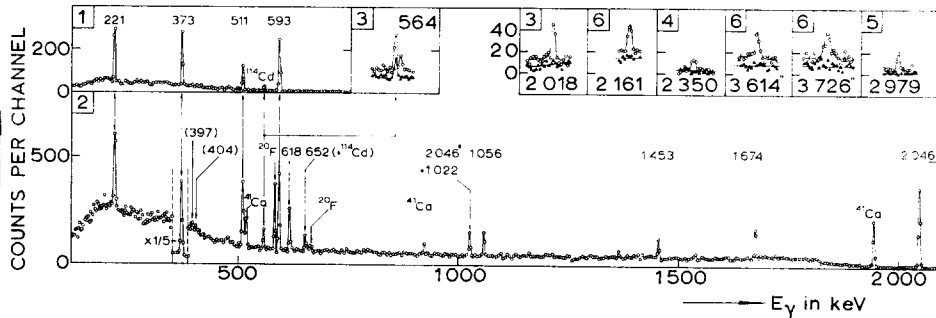


Fig. 2. Gamma-gamma coincidence spectra of  $^{43}\text{Ca}$ . The spectra are labelled according to the number of the window in the NaI channel (see table 4). For spectra coincident with windows 3-6, only those peaks are shown, which were not observed in the spectra coincident with the preceding window (indicated by triangles). Here the energy scale corresponds to 2.44 keV per channel.

cascades between the capturing state and the ground state, for which the sum of the energies of the constituent  $\gamma$ -lines equals the  $Q$ -value to within the standard deviation, and for which the energies of intermediate levels differ by less than one standard

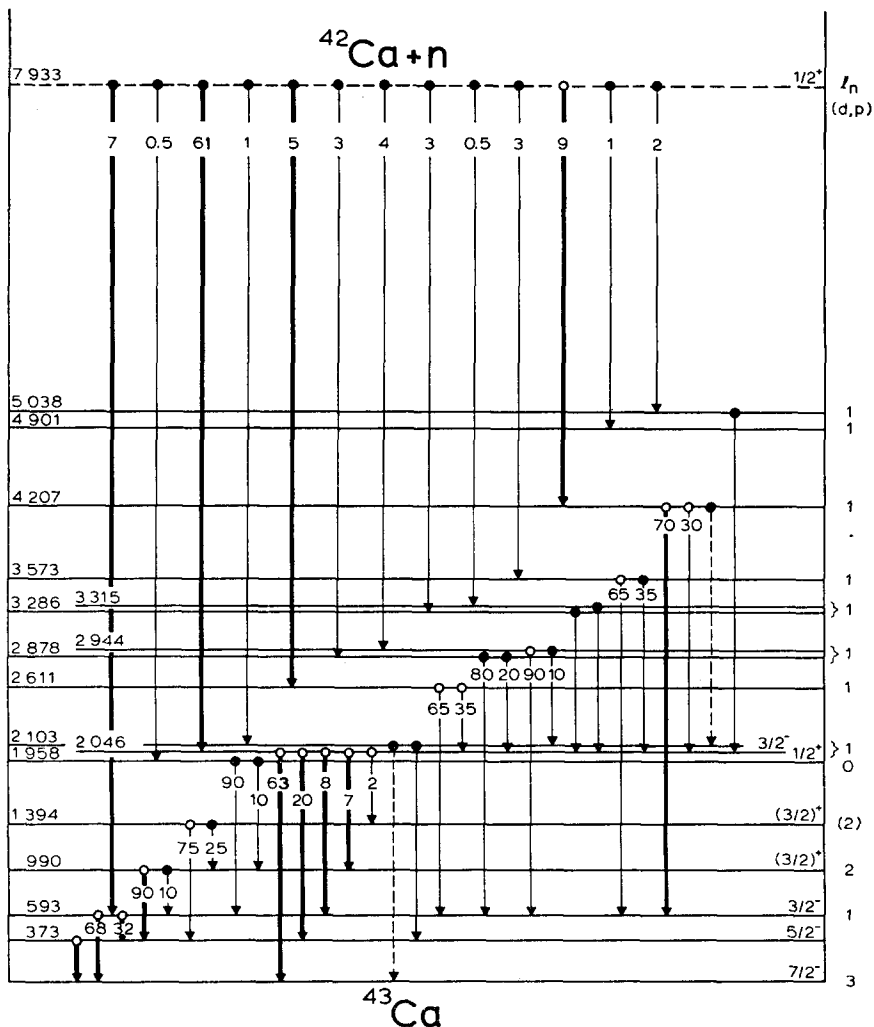


Fig. 3. Decay scheme of  $^{43}\text{Ca}$ . Here the total intensity of primary  $\gamma$ -rays is normalized to 100. For the bound levels the branching ratios are given. The  $\gamma$ -transitions, which were observed in coincidence are indicated by arrows starting with open circles. The  $\gamma$ -line at  $E_\gamma = 2103$  keV can be fitted in two ways into the decay scheme, as indicated by dotted lines. The  $J^\pi$  and  $I_n$  values are from ref. <sup>2)</sup>.

deviation from those found in the literature <sup>5,8)</sup>. The results of the  $\gamma$ - $\gamma$  coincidence measurements were useful to reject non-realistic cascades indicated by the program. Altogether 42 of the 47 observed  $\gamma$ -lines have been placed into the level scheme. The unexplained  $\gamma$ -lines are very weak. A few  $\gamma$ -rays could be fitted into the level scheme

at two different positions. In column 3 of table 3 the most likely interpretation has been given. Alternatives are indicated in footnotes.

TABLE 4  
Results of  $\gamma$ - $\gamma$  coincidence measurements

Nr.	Gate (MeV)	$E_\gamma$ (MeV) <sup>a)</sup>	Coincident $\gamma$ -rays ( $E_\gamma$ in keV)
1	6.75-7.15	7.34 <sup>b)</sup>	221, 373, 593
2	5.70-6.10	5.89	(397), (404), 618, 652, 1022, 1056, 1453, 1674, 2046
3	5.15-5.55	5.32	564, 2018
4	4.70-5.10	4.99	2350
5	4.10-4.50	4.36	2979
6	3.55-3.95	3.73	2161, 3614
		3.61	3726

<sup>a)</sup> Most prominent  $\gamma$ -transition in gate.

<sup>b)</sup> Gate on single-escape peak.

TABLE 5  
Excitation energies of  $^{43}\text{Ca}$  levels and consistency test of the decay scheme

$E_x$ (keV)		$Q$ -value <sup>b)</sup> (keV)	Intensity in	Intensity out
this work	other work <sup>a)</sup>			
0	0		100 $\pm$ 6	
372.7 $\pm$ 0.2	372.9 $\pm$ 0.5	7933.0 $\pm$ 0.8	32 $\pm$ 2	38 $\pm$ 4
593.4 $\pm$ 0.2	593.4 $\pm$ 0.4	7933.1 $\pm$ 0.9	26 $\pm$ 2	32 $\pm$ 2
990.4 $\pm$ 0.3	990.2 $\pm$ 0.4	7932.7 $\pm$ 0.8	4.9 $\pm$ 0.7	7.5 $\pm$ 0.7
1394.4 $\pm$ 0.5	1394.5 $\pm$ 0.5	7932.2 $\pm$ 1.2	0.9 $\pm$ 0.5	1.9 $\pm$ 0.4
1958.2 $\pm$ 0.5	1957 $\pm$ 4	7932.9 $\pm$ 1.9	0.6 $\pm$ 0.3	1.7 $\pm$ 1.0
2046.3 $\pm$ 0.2	2048 $\pm$ 5	7932.8 $\pm$ 0.5	60 $\pm$ 8	60 $\pm$ 5
2102.9 $\pm$ 0.5	2095 $\pm$ 5	7931.6 $\pm$ 1.6	1.2 or 2.4	2.4 or 1.2
2610.8 $\pm$ 0.4	2607 $\pm$ 5	7933.1 $\pm$ 1.1	4.1 $\pm$ 0.6	4.3 $\pm$ 0.6
2878.2 $\pm$ 0.4	2880 $\pm$ 5	7933.4 $\pm$ 1.3	2.4 $\pm$ 0.4	1.8 $\pm$ 0.5
2943.6 $\pm$ 0.4	2947 $\pm$ 5	7933.0 $\pm$ 0.9	3.6 $\pm$ 0.5	2.8 $\pm$ 0.4
3286.1 $\pm$ 0.5	3293 $\pm$ 6	7932.0 $\pm$ 1.4	2.4 $\pm$ 0.5	1.0 $\pm$ 0.2
3315.4 $\pm$ 0.5	3314 $\pm$ 10	7932.2 $\pm$ 1.1	0.6 $\pm$ 0.3	0.7 $\pm$ 0.2
3572.6 $\pm$ 0.5	3566 $\pm$ 10	7932.1 $\pm$ 1.0	2.9 $\pm$ 0.4	1.9 $\pm$ 0.4
4207.2 $\pm$ 0.5	4196 $\pm$ 10	7933.1 $\pm$ 0.7	8.3 $\pm$ 1.2	6.8 or 8.0
4901.3 $\pm$ 1.1	4897 $\pm$ 10		1.1 $\pm$ 0.3	
5037.8 $\pm$ 0.5	5028 $\pm$ 10	7934.1 $\pm$ 1.2	2.0 $\pm$ 0.3	0.6 $\pm$ 0.3
7932.7 $\pm$ 0.5 <sup>c)</sup>	7927.6 $\pm$ 4.8			88 $\pm$ 8

<sup>a)</sup> From Endt and Van der Leun <sup>2)</sup>, except for the first four excitation energies, which are from Larson and Gordon <sup>6)</sup>.

<sup>b)</sup> The  $Q$ -values are calculated from the energies of prominent  $\gamma$ -rays, cascading through the level with the  $E_x$  given in column 1.

<sup>c)</sup> Capturing state.

The consistency of the decay scheme can be tested by calculating the  $Q$ -values from different  $\gamma$ -cascades and by checking the intensity balance for each level. The result is shown in table 5, together with a comparison of the excitation energies from other



work. In general the agreement between the columns "intensity in" and "intensity out" is satisfactory, whereas the  $Q$ -values calculated from different cascades agree very well. The sum of the intensities of the primary  $\gamma$ -lines is  $88 \pm 8\%$  of the total intensity reaching the ground state. This might indicate (as mentioned above) that some weak primary  $\gamma$ -lines have not been observed.

The excitation energies, listed in table 5, and the  $Q$ -value for the  $^{42}\text{Ca}(n, \gamma)$  reaction were calculated with a least-squares method, which utilizes all the information from the decay scheme. The errors in  $E_x$  and  $Q$  have been enlarged in order to include a possible systematic error (estimated to be 0.3 keV in  $Q$ ). The value for the neutron-separation energy was determined as  $Q = 7932.7 \pm 0.5$  keV, in agreement with, but more accurate than that from the 1964 mass table <sup>24</sup>),  $Q = 7927.6 \pm 4.8$  keV.

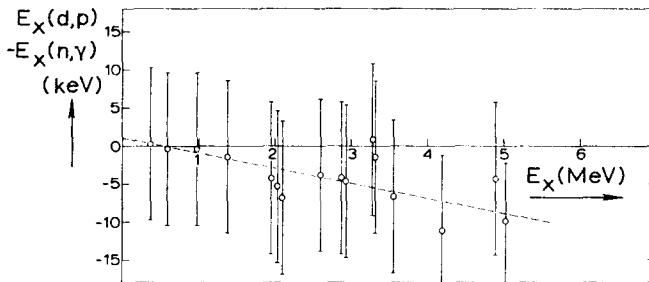


Fig. 4. The differences between the excitation energies from the (d, p) work <sup>8</sup>) and the present (n,  $\gamma$ ) work, as a function of  $E_x$ .

The differences between excitation energies from the (d, p) work <sup>8</sup>) and the (n,  $\gamma$ ) work, as a function of  $E_x$ , are plotted in fig. 4. The (d, p) values are systematically too low, the difference increasing with  $E_x$ , although the maximum deviation remains within the stated error.

TABLE 6  
Comparison of branching ratios observed in this and other work

Transition ( $E_x$ in keV)	Branching ratio (%)		
	this work	other work	ref.
593 $\rightarrow$ 0	$68 \pm 5$	$77 \pm 7$	<sup>5)</sup>
593 $\rightarrow$ 373	$32 \pm 5$	$23 \pm 7$	<sup>5)</sup>
990 $\rightarrow$ 0		0.3	<sup>25)</sup>
990 $\rightarrow$ 373	$90 \pm 5$	$78 \pm 7$	<sup>5)</sup>
990 $\rightarrow$ 593	$10 \pm 5$	$22 \pm 7$	<sup>5)</sup>
1394 $\rightarrow$ 0		<sup>a)</sup>	
1394 $\rightarrow$ 373	$75 \pm 15$	$78 \pm 8$	<sup>5)</sup>
1394 $\rightarrow$ 593		$6 \pm 2$	<sup>5)</sup>
1394 $\rightarrow$ 990	$25 \pm 15$	$16 \pm 6$	<sup>5)</sup>

<sup>a)</sup> Transition observed in  $\beta^-$  decay of  $^{43}\text{K}$  by Larson and Gordon <sup>6)</sup>.

The branching ratios for the levels excited in the  $^{42}\text{Ca}(n, \gamma)$  reaction are given in the decay scheme (fig. 3). Errors in the branchings may be deduced from table 3. In table 6 the branching ratios observed in this and other work are compared. The agreement is good.

### 5. Discussion

The  $(n, \gamma)$  reactions on the even calcium isotopes  $^{40}\text{Ca}$ ,  $^{42}\text{Ca}$  and  $^{44}\text{Ca}$ , in particular those on the latter two isotopes, show a great similarity. In these reactions a remarkable correlation exists between the  $(d, p)$  strengths  $(2J+1)S_n$  and the relative  $(n, \gamma)$  strengths  $I_\gamma/E_\gamma^3$  for primary  $\gamma$ -rays, leading to the same final states [ref. <sup>4</sup>] and fig. 5]. The correlation coefficients, defined in ref. <sup>4</sup>), for these reactions have been

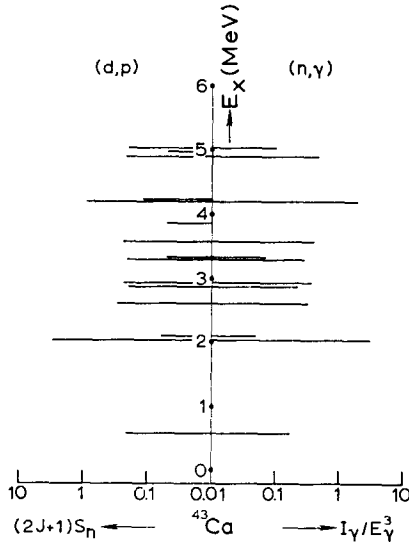


Fig. 5. Comparison between the  $(d, p)$  and  $(n, \gamma)$  strengths for  $l_n = 1$  levels in  $^{43}\text{Ca}$ . The  $(2J+1)S_n$  values are from ref. <sup>8</sup>). The quantity  $I_\gamma/E_\gamma^3$  has been normalized such that its value equals that of  $(2J+1)S_n$  for the level with the largest  $(d, p)$   $l_n = 1$  strength.

calculated as +0.59, +0.93 and +0.91, respectively. Most of the observed primary  $\gamma$ -transitions proceed to  $l_n = 1$  levels. A very prominent feature of the decay of the  $^{41}\text{Ca}$ ,  $^{43}\text{Ca}$  and  $^{45}\text{Ca}$  isotopes is the existence of a primary  $\gamma$ -ray with an intensity of more than 50 %, feeding a low-lying  $J^\pi = \frac{3}{2}^-$  state.

The low-lying positive-parity states in these odd calcium isotopes are weakly excited with a transition probability which decreases with the number of neutrons. This was also observed in the  $(d, p)$  work for the neutron strengths of the  $1d_{\frac{3}{2}}$  hole states [refs. <sup>26,27</sup>], and explained by assuming that the amplitudes of hole-state components in the ground state wave functions of the even calcium isotopes decrease with increasing neutron excess.

This correspondence between the (n,  $\gamma$ ) and (d, p) reactions gives some reason to expect a contribution of direct capture to the reaction mechanism of the (n,  $\gamma$ ) process. However, the theoretical arguments for such a conclusion are rather weak, since the thermal-neutron cross sections are larger than one should expect for direct capture<sup>28</sup>). Nor is it excluded that the compound-nucleus process plays a part in the (d, p) reaction<sup>29</sup>) at  $E_d = 7$  MeV.

In the following some properties of levels in  $^{43}\text{Ca}$ , which are excited in the (n,  $\gamma$ ) process, will be discussed.

### 5.1. THE ODD-PARITY LEVELS AT LOW EXCITATION ENERGIES

The main components of the wave functions of the  $E_x = 0, 373, 593$  and 2046 keV states seem to be well described by the shell-model configurations  $1f_{7/2}^3$  and  $1f_{7/2}^2 2p_{3/2}$  [ref. <sup>13</sup>)]. This has been confirmed by several authors who used more complex configuration spaces<sup>12,14-16</sup>).

The experimental spin assignments for these levels as given in the decay scheme (fig. 3) are from ref. <sup>2</sup>). The  $J(2046 \text{ keV}) = \frac{3}{2}$  assignment was obtained<sup>31</sup>) from the  $J$ -dependence of (d, p) angular distributions. This assignment is confirmed in the present work, since a strong transition from this level to  $^{43}\text{Ca}(0)$  with  $J^\pi = \frac{7}{2}^-$  was observed in coincidence with the  $E_\gamma = 5886$  keV  $\gamma$ -ray. The coincidence resolving time was  $2\tau = 50$  ns, which rules out the possibility of an M3 transition to the ground state (Weisskopf estimate:  $\tau_m(\text{M3}) = 4.4 \mu\text{s}$ ). Consequently, the spin for the  $l_n = 1$  level at  $E_x = 2046$  keV must be  $J = \frac{3}{2}$ . Analogous reasoning confirms that  $J^\pi = \frac{3}{2}^-$  for  $^{43}\text{Ca}(2)$ .

The E2 branchings of both  $J^\pi = \frac{3}{2}^-$  states to  $^{43}\text{Ca}(0)$  are relatively large. A possible explanation for this effect might be that the competitive M1 transitions are forbidden. This should be true if the low-lying odd-parity states were pure  $1f_{7/2}^3$  states. The M1 transition rates for transitions between these states were calculated by Zamick and Ripka<sup>16</sup>), who used an extended configuration space. They found probabilities of  $7 \times 10^{-4}$ ,  $6 \times 10^{-5}$  and  $7 \times 10^{-7}$  W.u. for the  $593 \rightarrow 373$ ,  $2046 \rightarrow 373$  and  $2046 \rightarrow 593$  keV transitions, respectively, which indicates that these transitions must contain appreciable E2 components.

The E2 transitions of the lowest  $J^\pi = \frac{3}{2}^-$  states in  $^{45}\text{Ca}$  towards the ground state are much weaker than those in  $^{43}\text{Ca}$ . Possibly E2 radiation is favoured in the case of  $^{43}\text{Ca}$ , due to polarization of the nuclear core, which is more prominent for  $^{43}\text{Ca}$  than for  $^{45}\text{Ca}$ .

### 5.2. THE ODD-PARITY LEVELS AT HIGHER EXCITATION ENERGIES

Shell-model calculations for the higher  $l_n = 1$  states have not been very successful. Since the number of observed  $l_n = 1$  states is quite large, the configuration space must be correspondingly large. Recently, McGrory and Wildenthal<sup>33</sup>) performed calculations in which all four f-p shell single-particle orbits were included. An excitation energy of  $E_x = 3.12$  MeV was calculated for the lowest  $J^\pi = \frac{1}{2}^-$  state in  $^{43}\text{Ca}$ . From

the work of Gerace and Green<sup>32)</sup> and Zamick<sup>30)</sup> it is evident that also configurations with two holes in the  $1d_{3/2}$  shell will contribute significantly.

Some very tentative spin assignments follow from the (d, p) angular-distribution  $J$ -dependence at  $E_d = 7$  MeV [ref. 8)]:  $J(2.10) = (\frac{3}{2})$ ,  $J(2.61) = (\frac{1}{2})$ ,  $J(2.88) = (\frac{1}{2})$ ,  $J(2.94) = (\frac{3}{2})$ ,  $J(3.29) = (\frac{3}{2})$ ,  $J(3.57) = (\frac{3}{2})$ ,  $J(4.21) = (\frac{1}{2})$ , and  $J(4.90) = (\frac{1}{2})$ . The  $\gamma$ -decay from these states gives little additional information about the spins of these levels. The level at  $E_x = 2103$  keV de-excites to  $^{43}\text{Ca}(1)$  with  $J^\pi = \frac{5}{2}^-$ , which gives a weak indication that this level has  $J^\pi = \frac{3}{2}^-$ . Unfortunately the  $E_\gamma = 2103$  keV  $\gamma$ -ray has not been uniquely fitted into the level scheme.

It is a pleasure to express our appreciation to Professor P. M. Endt for his stimulation of this work and valuable criticism. The advice of Dr. C. van der Leun is acknowledged. We thank A. A. P. Smit for the assistance in the analysis of the data obtained with the  $6.5 \text{ cm}^3$  Ge(Li) detector.

This investigation was partly supported by the joint program of the "Stichting voor Fundamenteel Onderzoek der Materie" and the "Nederlandse Organisatie voor Zuiver Wetenschappelijk Onderzoek". The cooperation with the "Stichting Reactor Centrum Nederland" was appreciated.

### References

- 1) F. P. Cranston, D. H. White and A. J. Smith, *Bull. Am. Phys. Soc.* **9** (1964) 717
- 2) P. M. Endt and C. van der Leun, *Nucl. Phys.* **A105** (1967) 1
- 3) H. Gruppelaar and P. Spilling, *Nucl. Phys.* **A102** (1967) 226
- 4) H. Gruppelaar, P. Spilling and A. M. J. Spits, *Nucl. Phys.* **A114** (1968) 463
- 5) C. Chasman, K. W. Jones and R. A. Ristinen, *Phys. Rev.* **169** (1968) 911
- 6) R. E. Larson and C. M. Gordon, *Bull. Am. Phys. Soc.* **13** (1968) 697
- 7) T. A. Belote, J. H. Bjerregaard, O. Hansen and G. R. Satchler, *Phys. Rev.* **138** (1965) B1067
- 8) W. E. Dorenbusch, T. A. Belote and O. Hansen, *Phys. Rev.* **146** (1966) 734
- 9) O. Lynen, thesis, Heidelberg (1967)
- 10) W. E. Dorenbusch, F. T. Dao, J. Rapaport and T. A. Belote, *Phys. Lett.* **26B** (1968) 148
- 11) S. M. Smith and A. M. Bernstein, *Nucl. Phys.* **A113** (1968) 303
- 12) B. J. Raz and M. Soga, *Phys. Rev. Lett.* **15** (1965) 924
- 13) T. Engeland and E. Osnes, *Phys. Lett.* **20** (1966) 424
- 14) P. Federman and I. Talmi, *Phys. Lett.* **22** (1966) 469
- 15) G. Ripka and L. Zamick, *Phys. Lett.* **23** (1966) 350
- 16) L. Zamick and G. Ripka, *Nucl. Phys.* **A116** (1968) 234
- 17) A. E. L. Dieperink and P. J. Brussaard, *Nucl. Phys.* **A106** (1968) 177
- 18) G. van Middelkoop and P. Spilling, *Nucl. Phys.* **72** (1965) 1
- 19) P. Spilling, H. Gruppelaar and P. C. van den Berg, *Int. Symp. on Nucl. Electronics, Versailles* (1968) Part II, Contr. 140
- 20) F. P. Cranston, P. B. Snow and D. H. White, *Bull. Am. Phys. Soc.* **11** (1966) 909
- 21) D. J. Hughes and R. B. Schwartz, *Brookhaven Nat. Lab. Rep.*, BNL-325 (1968) 6
- 22) F. Ajzenberg-Selove and T. Lauritsen, *Nucl. Phys.* **11** (1959) 265
- 23) W. R. Kane and R. Mariscotti, *Nucl. Instr.* **56** (1967) 189
- 24) J. H. Mattauch, W. Thiele and A. H. Wapstra, *Nucl. Phys.* **67** (1965) 32
- 25) R. E. Holland, F. J. Lynch and A. M. Mann, *Bull. Am. Phys. Soc.* **10** (1965) 119
- 26) J. Rapaport, W. E. Dorenbusch and T. A. Belote, *Phys. Rev.* **156** (1967) 1255
- 27) T. A. Belote, W. E. Dorenbusch and J. Rapaport, *Nucl. Phys.* **A120** (1968) 401
- 28) C. K. Bockelman, *Nucl. Phys.* **13** (1959) 205

- 29) A. Denning, J. G. B. Haigh and C. Brown, *Phys. Lett.* **27B** (1968) 159
- 30) L. Zamick, *Ann. of Phys.* **47** (1968) 182
- 31) J. P. Schiffer, Argonne Nat. Lab. Rep. ANL-6878 (1964) 145
- 32) W. J. Gerace and A. M. Green, *Nucl. Phys.* **93** (1967) 110
- 33) J. B. McGrory and B. H. Wildenthal, *Phys Lett.* **26B** (1968) 237
- 34) H. W. Taylor, N. Neff and J. D. King, *Phys. Lett.* **24B** (1967) 659
- 35) C. M. Lederer, J. M. Hollander and I. Perlman, *Table of isotopes*, 6th ed., Appendix II (Wiley, New York, 1967)
- 36) P. Spilling, H. Gruppelaar, H. F. de Vries and A. M. J. Spits, *Nucl. Phys.* **A113** (1968) 395